Estimate Long-term Impact on Battery Degradation by Considering Electric Vehicle Real-world End-use Factors

Shiqi Ou[a,*]

a. Buildings and Transportation Science Division, Oak Ridge National Laboratory, 2360 Cherahala Blvd, Knoxville TN 37932, USA. Email: ous1@ornl.gov (S. Ou, corresponding author)

Abstract

Many estimates of battery capacity degradation are based on accelerated lab tests that involve charge-discharge cycles or rely on data or electrochemical modeling. These methods are reasonable for technology benchmarking but rarely consider real-world end-use factors. To address this issue, this study develops the Battery Run-down under Electric Vehicle Operation (BREVO) model. It links the driver's travel pattern to physics-based battery degradation and powertrain energy consumption models. The model simulates the impacts of charging behavior, charging rate, driving patterns, and multiple energy management modules on battery capacity degradation. It finds that, over a 10-year timespan, firstly, for a random driver situated in the New England area, daily direct-current fast charging (60kW) could lead to up to 22% less battery capacity when compared to daily Level-1 charging (1.8kW). Second, the battery thermal management system can delay battery degradation by approximately 0.5% in the New England area. Third, warmer ambient temperatures enhance BEV battery usage. The model indicates that the battery capacity in the Los Angeles area is 6% higher than that in the New England area. The BREVO model provides crucial information for consumers and BEV manufacturers on range anxiety, BEV battery design, and decision support of battery warranty.

Keywords: Battery capacity degradation, Driving patterns, Electric vehicle, Fast charging, Powertrain energy consumption

1. Introduction

The increasingly strict fuel economy and emission standards in major vehicle markets have prompted the production of internal combustion engine vehicles with higher hybridization levels or plug-in electric vehicles (PEVs) [1]. As a result, more than 6.6 million of PEVs were sold globally in 2021 [2]. According to the policy scenario to achieve the climate goals of the Paris Agreement, it is expected that the global electric vehicle stock will reach nearly 140 million vehicles and account for 7% of the global vehicle fleet by 2030 [3]. In particular, the Biden administration has pledged to reach net-zero greenhouse gas emissions no later than 2050 [4], with 100% clean electricity expected to be realized by 2035 [5]. This policy adjustment has shifted the product strategies of many auto manufacturers towards electric vehicles. For instance, Volvo, Volkswagen, and Stellantis have been implementing their electrification strategies [6–8]. In China, hundreds of Chinese companies, including those that dominate the internal combustion engine vehicle market, such as Dongfeng Auto and Shanghai Auto, are now competing in the BEV market [9].

However, the Achilles' heel of BEVs is its power source – the battery. Currently, the market is still searching for a low-cost battery that can provide a reliable electric driving range to consumers. The cell level of commercial lithium-ion batteries had an average specific energy of 200 Wh/kg in 2018, which is below the target of 500 Wh/kg specified by the U.S. Department of Energy (DOE) [10]. The DOE estimated the vehicle lithium-ion battery pack declined by 89% from 2008 to 2022, in which the cost is $153/kWh on a usable-energy basis [11]. Turcheniuk et al. claimed that further development of the electric vehicle market could be hindered by the lithium-ion battery since they believe that its cost and performance improvement progress is still

slower than the market demands [12]. Expansion of the car charging infrastructure in the U.S. is also needed to improve the convenience of using electric vehicles [13]. The U.S. DOE and Department of Transportation have announced plans to invest nearly $5 billion to support the new National Electric Vehicle Infrastructure (NEVI) Formula Program to create nationwide charging accessibility for BEVs [14]. Frequent and quick charging can extend the BEV's electric driving range, thereby reducing the range anxiety and the time costs for the BEV drivers [15]. Therefore, fast chargers (FC), capable of delivering 60 to 80 miles of range in 20 minutes of charging, are recommended for deployment, especially along heavy traffic corridors [16]. Many charging infrastructure publications have presumed that FC or extreme fast charging (xFC) would promote the adoption of electric vehicles and focus more on station siting selection and optimization [17,18]. FC, and particularly xFC, has been known to accelerate battery degradation under certain conditions [19]. However, it is not well understood how often these conditions may occur in the real world, possibly discouraging utilization or forcing tradeoffs between battery life and range extension.

A comprehensive understanding of real-world battery performance and end-use behavior factors such as charging power, ambient temperature, and driver patterns is crucial for accurately estimating battery lifetime and avoiding potential misconduct on battery uses. While many battery testing results are obtained from accelerated lab tests under extreme conditions, such results may not accurately reflect on-road performance [20,21]. Some lab-based battery testing studies indicate that battery capacity degradation is slower with a smaller state-of-charge (SOC) window during charge-discharge cycles [20]. Existing battery lifetime models, such as the Battery Lifetime Analysis and Simulation Tool (BLAST) [22], consider some of these

relationships, but tend to focus on degradation factors and lack clear linkages to end-use factors, especially travel profiles and charging activities [23]. In addition, some buyers are concerned that the BEV battery life may not exceed 65,000 miles before requiring replacement [24]. On the other hand, the BEV leasing company Tesloop has reported that its Tesla Model S vehicles have been driven over 400,000 miles without significant battery capacity degradation [25], although it is not yet clear if the smaller depth of discharges (DoDs) is the explanation. Therefore, there is a research gap in associating battery lifetime validation through lab tests or models with real-world evaluations by users. The validity of the hypotheses mentioned above can potentially affect total ownership cost calculations as well as consumer sentiments and supplier outlooks regarding BEV products.

The degradation or lifetime of a BEV's battery can be impacted by various end-user factors such as working (ambient) temperature, frequencies of battery charging-discharging, and powertrain energy consumption control modules [26]. It is widely known that the capacity of the lithium-ion battery or the lithium-iron-phosphate battery decreases substantially as temperature drops, and this is primarily due to increased electrolyte viscosity at low temperatures [20,27]. Moreover, the previous results show that battery degradation occurs more quickly when the testing temperature is above its normal operating temperature [28]. Therefore, the vehicle-to-grid technology could hurt the use of BEV if battery impact is considered [29]. To save energy consumption and account for various physical factors impacting the BEV's battery operation, the BEV is equipped with several powertrain energy consumption modules, such as the regenerative braking system (RBS) [30], the heating, ventilation, and air conditioning (HVAC) system [31], and the battery thermal management system (BTMS) [31] to improve the energy efficiency.

These energy consumption modules could also affect battery degradation from a long-run perspective.

The objective of this study is to fill a research gap by associating BEV battery degradation models/experiments with BEV simulations under the real-world long-term driving profile. The study aims to estimate the potential impacts of major end-user factors such as driving pattern, charging behavior, ambient temperature, charging power, and powertrain energy consumption control modules on the BEV battery life. The powertrain energy consumption control modules discussed in this study include RBS, HVAC, and BTMS. The study links existing lab-based relationships to real-world end-user behavior data and generates impactful insights on BEV battery life. This approach is rarely comprehensively conducted in other previous studies, as listed in Table 1. Considering the large-scale installations of xFCs and the plans for vehicle-to-grid technology, the negative influence of xFC or other charging behaviors on battery degradation could potentially increase the ownership costs of BEVs. As lithium-ion batteries dominate the BEV market, this study discusses the impacts of lithium-ion batteries only instead of other battery chemistry materials.

Table 1. Summary of recent literature on BEV battery degradation model.

Studies	**Contributions**	**Limits**
Zhao et al. 2023 [32]	It develops a stacking ensemble machine learning model to estimate the state of health of commercial lithium iron phosphate/graphite cells.	The study cannot be applied to all real-world scenarios, such as uncontrolled partial charging cycles, fast charging modes, and complex low-temperature aging mechanisms.
Neubauer et al. 2014 [22]	This study is one of the pioneers that creates a systematic powertrain and battery model to understand	It lacks clear linkages to end-use factors, especially travel profiles and charging activities.

	battery degradation and lifetime.	
Jafari et al. 2018 [33]	This study builds a model for evaluating electric vehicle battery aging by considering both real-world Daily driving and vehicle-to-grid services.	This study has comprehensively considered both the battery and real-world end-user factors. However, the model for the powertrain system is simplified.
Severson et al. 2019 [34]	This work highlights the promise of combining deliberate data generation with data-driven modeling to predict the behavior of complex battery dynamical systems.	This work focuses on a data-driven model to simplify the complex electrochemical relations in the battery system. It has not examined the model reliability when the end-user factors on the real-world road are considered.

This paper consists of five sections. Section one provides background, discusses some of the literature on BEV battery technology and its degradation impact factors, and presents research motivations and objectives. Section two summarizes the major end-use factors determining the battery lifetime and describes the review of data and literature on existing lab-based relationships. Section three provides modeling assumptions and methodology for building the Battery Run-down under the Electric Vehicle Operation (BREVO) model. Section four quantifies the impacts of driver-end factors on battery life in the simulated real-world travel pattern by scenarios. The last section provides summaries and conclusions.

2. End-use Factors Impacting the Battery Lifetime

Battery lifetime is commonly measured by the number of charge-discharge cycles before the battery capacity is degraded to 80% of its original capacity. However, the testing method for battery charge-discharge cycles is based on accelerated tests with deep discharge and full recharge cycles [35]. Henschel et al. extended the battery performance to the on-road test which lasts for minutes and hardly implicates long-term impacts [36]. These methods are reasonable for

technology benchmarking but do not represent real-world end-user factors and therefore are inadequate for informing consumers and BEV manufacturers, such as the total cost of ownership, range anxiety over vehicle lifetime, BEV's electric range design, and battery warranty offered. Existing research has identified some quantified relationships between battery degradation and some end-use factors such as daily driving patterns [33]. This study reviews the end-use factors such as driving pattern, terrain, charging behavior, ambient temperature, charging power, and calendar degradation, which are summarized in Table 2.

Table 2. Summary of end-user factors on battery degradation.

End-use factor	**Key degradation factor**	**Existing studies**	**Battery lifetime conflicts**
Driving pattern	Depth of discharge, discharging rate, charging rate, film resistance	[33,37]	Battery cost, range anxiety, energy cost
Terrain		[38]	Battery cost, range anxiety, energy cost
Charging behavior		[33]	Range anxiety, energy cost
Charging power		[20,39,40]	Value of time, range anxiety
Ambient temperature	Thermal management, film resistance	[20,41]	Thermal management capital cost, range loss, energy cost
Calendar degradation	Storage SOC	[39]	Range anxiety

The estimate of the BEV battery lifetime or the utilization of FC should be consistent with the use frequency of fast/slow charging and discharging/recharging ratio of the BEV users while considering their travel patterns. To maintain the battery capacity and extend the battery lifetime, several potential barriers summarized in Table 3 must be conquered [19]. Through simulation in the BREVO model, this study estimates and compares the impacts of different charging patterns, vehicle usage, and locations on the battery capacity of a sedan-sized BEV.

Table 3. Solutions to protect the battery during xFC.

Factors that damage the battery capacity/life	Current solution	Reality	Potential solution
Frequent heavy charging power load	BMS controls the SOC between 20% and 80%.	Most trip distances are short.	Based on the driver travel patterns to more accurately project potential discharge levels of BEV's battery.
Battery lithium plating	Change to a thinner electrode	Thinner electrodes increase battery costs and lower energy density, which could result in more cells.	A larger scale of battery manufacturing to lower cost, or development of new electrode/electrolyte materials and electrode architecture to boost lithium-ion transport
Overheating	BMS detects the temperature.	Drivers can choose to use FC & xFC.	Based on the driver's travel patterns to help to determine what charge rate and when to charge their EVs.

2.1. Depth of discharge

The way of using a BEV could change the level of battery degradation or the battery life. Firstly, the discharge cycles can highly correlate to the depth of discharge (DoD) which describes the SOC window. Table 4 indicates common aging trends of lithium-ion batteries on DoD. In this table, two lithium-ion battery products are used as examples. The first example is a lithium-ion battery product with nickel manganese cobalt oxide (NMC) as the cathode, and the second example is a lithium-ion battery product with iron phosphate as the cathode material (LFP). Although the exact numbers of discharge cycles vary by test environment or battery materials, a heavy load of charge and discharge can result in less number of charge-discharge cycles; and a partial discharge can extend the life span of the lithium-ion batteries [42]. That's why the battery management system (BMS) in BEVs automatically limits the SOC between 20%

and 80% [43]. This study uses the trend for the DoD and the discharge cycles of the NMC battery shown in Table 4 to quantify the relation of these two variables, and it describes this relation by fitting it with a power equation (R-square = 0.9946), as shown by Eqn. (1).

$$n = 302.4 \times DoD^{-1.264} \quad (1)$$

Where n is the number of discharge cycles of a lithium-ion battery in BEVs; and DoD is the depth of discharge. For example, 80% of DoD signifies that the difference between the SOC level at the beginning of discharge and the SOC level at the end of discharge is 80%. It is known that the number of discharge cycles depends on many variables other than the DoD, and this study focuses on the overall degradation of battery use under long-term electric vehicle operations; thus, this study purposely uses a fitting to simplify this part of the simulation, which can be expanded in the future.

Table 4. Relationship between DoD and discharge cycle for two lithium-ion battery products as examples* [42].

Depth of discharge (DoD)	**Discharge cycles**	
	An NMC Battery	**An LFP Battery**
100%	~300	~600
80%	~400	~900
60%	~600	~1,500
40%	~1,000	~3,000
20%	~2,000	~9,000
10%	~6,000	~15,000

* The terms - “NMC” and “LFP” used in this table do not imply that the discharge cycles will be affected only by the cathode.

Meanwhile, the battery’s DoD in the real world might not be consistent with the battery life cycle test in the laboratory. For example, to evaluate battery capacity degradation and understand the impact of battery expansion, Mohtat et al. tested the discharge cycles under

different DoDs [44], which clearly shows the correlation between different battery features. On the other hand, according to studies on driver travel patterns in the U.S. and China, the distance of most driving trips is less than 20 miles [45,46]. If BEV drivers charge frequently after the end of their trips, the DoD of BEV batteries in most driving scenarios is smaller, and thus, the vehicle battery could persist much longer than what we expect based on the lab-based battery testing which often implicates only thousands of cycles. Therefore, the real-world travel patterns could be a remarkable factor impacting the battery lifetime, and more recent battery research studies have considered the simulation or test with referring to the real-world driving cycles [23,47].

2.2. Charging rate

A higher charging rate on a lithium-ion battery could cause problems such as lithium plating on the surface of the electrode, and this detriment varies as the combination of battery anode/cathode materials changes [48,49]. Therefore, the charging rate and the charging frequency are another type of use-end factor impacting the BEV's battery lifetime, especially faster charging with higher wattages, such as the Level 3 direct-current (DC) FC, Tesla Supercharger, and xFC, [14,19]. The charging levels and their features discussed in this study are shown in Table 5. The conventional DC FC provides voltage directly to the BEV battery via a DC connector, usually with a power of 50 kW and a voltage ranging from 208 V to 600 V [50]. The time to charge for 200 Miles by DC FC can be about 60 mins [19]. Tesla V3 Supercharger can deliver a peak of 240 kW of charging power, and a nearly consistent 72 kW of power depending on battery usage and age [51]. In addition, xFC defined by the DOE is the charger that can deliver a peak charging rate of 150–400 kW; the xFC can recharge a BEV in less than 10 mins and provide approximately 200 additional miles of electric range [19]. However, the xFC could potentially damage the lifespan of the BEV battery as internal heat generation could more

rapidly degrade the battery lifetime, although this can be regulated by BTMS [52]. In addition, the round-trip efficiency at xFC will also be lower and it would also cause the charging cost of xFC to be higher per usable watt-hour. What's more, the battery which is suitable for the xFC is more expensive than the general batteries in the market [19]. The high voltage and the high power of xFC require more improvement of the vehicle components such as the electric drive motor and the power electronics, and the installation of xFC infrastructure would be more expensive [19]. Therefore, the adoption of xFC could not be that simple: a larger scale of xFC adoption indicates higher upfront investment cost, and it could also bring extra potential permanent damage to batteries if these end-use factors are ignored.

Table 5. Charging types and features used in the scenarios.

Vehicle charger	Charging power (kW)	Charging voltage (V)	Charging efficiency	Charging price ($/kWh)
Level 1	1.8	120	0.85	0.13
Level 2	7.6	240	0.85	0.13
DC FC	60	480	0.85	0.26
xFC	400	800	0.85	0.52

To avoid the battery's permanent damage and battery degradation caused by the high voltage or overheating during fast charging, the major solution adopted by BEV manufacturers is to utilize a reliable BMS to reasonably distribute voltage for each cell in the battery pack. For example, for a Tesla vehicle, the charging power rate may vary due to battery charge level, current use of the supercharger, and extreme climate conditions, so it is very often that the charging time could be longer than the ideal expectation to ensure maximum driving range and battery safety [51]. At the same time, if we understand the driver's travel pattern and can design a method to inform the driver whether to charge their BEVs with Level 1-2 charger or FC &

xFC, we can not only prolong the use of batteries but also smartly save the investment on public charging facilities.

3. Method and Assumptions

3.1. The physical-based powertrain energy model

To understand the variations of the battery lifetime of BEVs under driving scenarios that simulate real-world long-term BEV usage, this study builds an Excel® VBA-based model, named BREVO to quantify the impacts of different vehicle- and driver- features. The BREVO model associates the transportation analysis of driving behaviors with the physical-based powertrain energy model. The structure of the physical-based energy flow model, which is used to quantify the vehicle-end features, is similar to other vehicle powertrain system models [20,22,30] The BREVO model consists of four components: (a) vehicle energy transfer module, (b) battery aging module, (c) battery electric-thermal module, and (d) charging module. The structure of the physical-based energy flow model is shown in Figure 1.

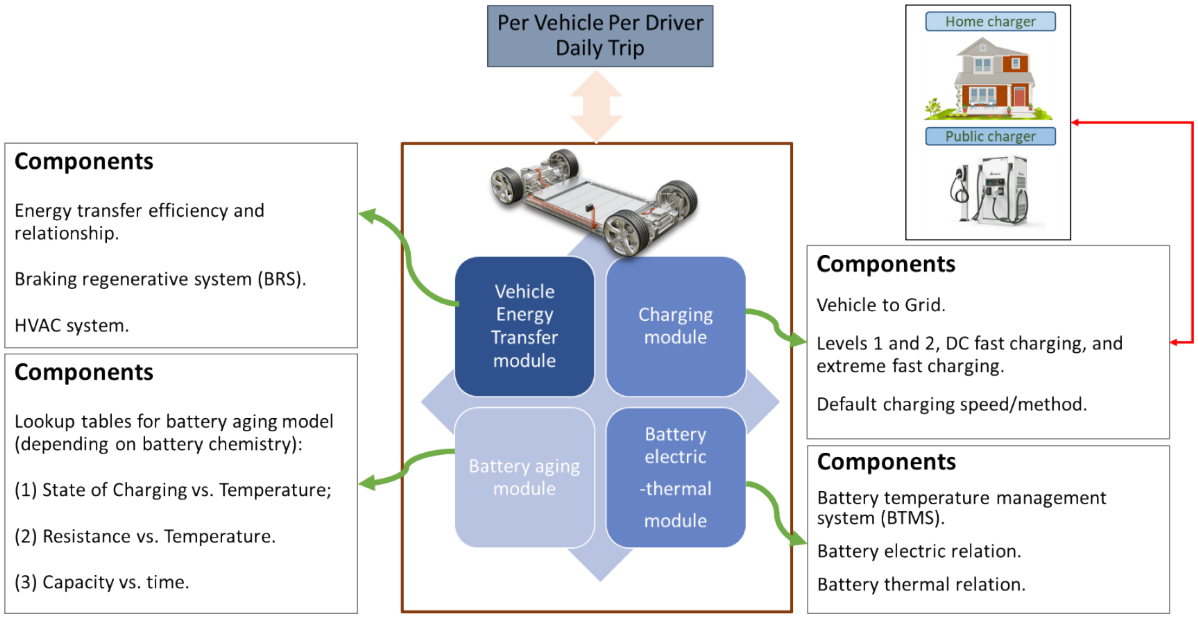

Figure 1. Structure of the physical-based powertrain energy model in BREVO.

3.1.1. Vehicle energy transfer module

The vehicle energy transfer module is a component of considering the BEV powertrain dynamics and integrating RBS and HVAC in the simulation. The vehicle kinetics and powertrain energy efficiency information are presented in Table 6. The battery provides the desired power to move the vehicle. Eqn. (2-6) shows the major relationships of the vehicle dynamics: the total force to move the vehicle (F_{pt}), the air drag force (F_d), the rolling resistance force (F_r), the grading force (F_g), and the acceleration force (F_t).

$$F_{pt} = F_d + F_r + F_g + F_a \tag{2}$$

$$F_d(t) = \frac{1}{2}\rho_{air}A_d c_d(v_c(t) - v_{wind})^2 \tag{3}$$

$$F_r(t) = c_r m_v g cos(\theta) \tag{4}$$

$$F_g(t) = m_v g cos(\theta) \tag{5}$$

$$F_a(t) = \sigma m_v a_{car}(t) \tag{6}$$

Where, $v_c(t)$ is the vehicle speed varying by time, and $a_{car}(t)$ is the vehicle acceleration varying by time. Accordingly, the energy to move the vehicle (W_{pt}, J) is shown in Eqn. (7).

$$\frac{dW_{pt}}{dt} = F_{pt}v_c(t) \tag{7}$$

Table 6. Vehicle powertrain and battery parameters.

Parameters	Units	Descriptions	Value
		Vehicle Powertrain	
A_d	m^2	Front area	2.130
c_d	-	Coefficient of aerodynamic resistance	0.350
c_r	-	Rolling resistance coefficient	0.015
f_{acc}	-	Accessory energy efficiency (energy consumed by accessory electronics etc.)	0.98

f_{pt}	-	Powertrain efficiency (energy flow direction is from the battery to the wheel)	0.90
f_{rbs}	-	Regenerative efficiency (Stored energy/braking energy)	0.63
g	m/s^2	Gravitational constant	9.810
m_v	kg	Vehicle gross weight	1,100.000
v_{wind}	m/s	Wind speed	0.000
θ	deg	Road inclination	0.000
σ	-	Correction coefficient of rotational inertia	1.300
ρ_{air}	kg/m^3	Air density	1.225
		Battery Basic	
C_{ini}	Ah	Battery initial capacity	198.5
P_d	kWh	Max deliverable energy	85
V_{max}	V	Max voltage	400
V_{min}	V	Min voltage	270
		Battery Thermal	
C_b	J/K	Heat capacity of the battery	101,771
C_c	J/K	Heat capacity of the vehicle cabin	182,000
f_{btms}		Coefficient of BTMS performance (ratio between BTMS heat transfer and BTMS energy demand)	0.9
K_{ab}	W/K	Effective heat transfer coefficient between ambient & battery system	4.343
K_{ac}	W/K	Effective heat transfer coefficient between ambient & vehicle cabin	22.600
K_{bc}	W/K	Effective heat transfer coefficient between battery system & vehicle cabin	3.468
K_{btms}	W/K	Effective heat transfer between battery and battery thermal management system	340
Q_{rad}	kW	Solar irradiance (default = 0)	0
$T_{b,up}$	°C	The temperature ceiling that BTMS is not working	30
$T_{h,up}$	°C	The temperature that HVAC removes heat from the vehicle cabin to the ambient	23.88
$T_{b,low}$	°C	The temperature bottom that BTMS is not working	10
$T_{h,low}$	°C	The temperature that HVAC adds heat from the ambient to the vehicle cabin	18.85

In addition, the RBS and the HVAC are common components in the BEV powertrain system and are also integrated in the BREVO model. For the RBS, it assumes that the braking energy is regenerated when the vehicle speed, v_c, is over 5 km/h (1.389 m/s) [53]. For simplification, the braking energy is stored in the battery system with a fixed efficiency - f_{rbs}, therefore, only a partial of the powertrain energy can be recycled back to the battery system.

The simulation of the HVAC system in this model is based on Neubauer et al. [54] and Maranville et al.'s work [55]. The HVAC determines the heat (Q_{hvac}, J) from or to the vehicle cabin. The working status of the HVAC depends on the temperature of the vehicle cabin (T_c): the heat transfer rate, $\frac{dQ_{hvac}}{dt}$, is 4 kW when $T_c > T_{h,up}$ (cooling); the heat transfer rate is -4.5 kW when $T_c < T_{h,low}$ (heating); and otherwise, the heat transfer rate is calculated by Eqn. (8).

$$\frac{dQ_{hvac}}{dt} = -1.7 \cdot (T_c + 273.15) + 500.4 \quad (8)$$

Where, $\frac{dQ_{hvac}}{dt}$ is positive when the heat is added from the ambient to the vehicle cabin and is negative when the heat is removed from the vehicle cabin to the ambient.

At the same time, the HVAC system is powered by the vehicle battery. The energy demand (W_{hvac}) for the HVAC system to work is determined by the size of heat transfer (Q_{hvac}) and the ratio of heat dissipation/electrical power intake (COP). The COP is 1.5 when the HVAC works for cooling, and the COP is 2.5 when the HVAC works for heating, as shown in Eqn. (8). The positive/negative sign of energy does not indicate the size but the energy flow direction.

$$\begin{cases} W_{hvac} = \frac{|Q_{hvac}|}{COP_{cooling}}, HVAC\ cooling, Q_{HVAC} < 0 \\ W_{hvac} = \frac{|Q_{hvac}|}{COP_{heating}}, HVAC\ heating, Q_{HVAC} \geq 0 \end{cases} \quad (8)$$

3.1.2. Battery aging module

The BEV battery aging in the BREVO model consists of two types of aging: calendar aging [56], and thermal aging [57]. Calendar aging is a degradation of a battery independent of charge-discharging cycling. This study summarizes the experiment data provided by Wikner et

al. [58] as a lookup table, as shown in Table 7, to derive the calendar aging rate (τ_c, %) by battery SOC and battery temperature. The interpolation method is adopted if the values are not in the table. The growth function, as shown in Eqn. (9), is used for fitting the relation between calendar aging rate and SOC value at a specific battery lifetime for 25 ℃ and 35 ℃ respectively.

$$\tau_c(SOC) = b \cdot m^{SOC} \quad (9)$$

Where, b and m are the fitting parameters for each specific battery lifetime. The calculation process for $\tau_{c,tgt}$ at SOC=SOC_{tgt}, battery temperature $T = T_{tgt}$, and battery lifetime L_{tgt}:

a) If the specific battery lifetime (L_{tgt}) is not in the lookup table, the calendar aging rate values for each SOC value (0.00, 0.15, 0.90, 1.00) will be firstly linearly interpolated based on the nearest two battery lifetime values, $L_{tgt,1}$ and $L_{tgt,2}$, in the lookup table.
b) Then, two growth functions will be fitted: one is the function of $\tau_{c@L_{tgt}@25C}(SOC)$ for battery temperature at 25 ℃, and the other is the function of $\tau_{c@L_{tgt}@35C}(SOC)$ at 35 ℃. Accordingly, $\tau_{c@L_{tgt}@SOC_{tgt}@25C}$ and $\tau_{c@L_{tgt}@SOC_{tgt}@35C}$ are calculated based on the growth functions, respectively.
c) Ultimately, $\tau_{c@L_{tgt}@SOC_{tgt}@T_{tgt}}$ is obtained through the linear interpolation between $\tau_{c@L_{tgt}@SOC_{tgt}@25C}$ and $\tau_{c@L_{tgt}@SOC_{tgt}@35C}$.

One benefit of this calculation is that the lookup table is simple and automatic to be expanded as more experimental data are achieved, and the estimate of the calendar aging rate will be more accurate.

Table 7. Relation between the calendar aging rate with SOC, battery lifetime, and battery temperature.

Calendar aging rate	SOC							
Battery temperature	25 ℃				35 ℃			
Battery lifetime (days)	0.00	0.15	0.90	1.00	0.00	0.15	0.90	1.00
0	100%	100%	99%	99%	100%	100%	99%	99%
200	100%	99%	97%	97%	100%	99%	96%	96%
400	100%	99%	96%	95%	100%	98%	95%	95%
600	100%	99%	95%	94%	100%	98%	91%	91%
800	100%	98%	94%	93%	100%	98%	91%	90%
1000	100%	98%	92%	92%	100%	97%	89%	88%
1200	100%	97%	91%	90%	100%	97%	87%	86%
1400	100%	97%	90%	89%	100%	97%	85%	83%
1600	100%	97%	89%	88%	100%	96%	83%	81%
1800	100%	96%	88%	87%	100%	96%	81%	79%
2000	100%	96%	87%	86%	100%	95%	79%	77%
2200	100%	96%	86%	85%	100%	95%	77%	75%
2400	100%	95%	85%	83%	100%	95%	75%	73%
2600	100%	95%	84%	82%	100%	94%	73%	71%
2800	100%	95%	83%	81%	100%	94%	71%	68%
3000	100%	94%	82%	80%	100%	93%	69%	66%
3200	100%	94%	81%	79%	100%	93%	67%	64%
3400	100%	93%	80%	78%	100%	93%	65%	62%
3600	100%	93%	79%	77%	100%	92%	63%	60%
3800	100%	93%	78%	76%	100%	92%	61%	58%
4000	100%	92%	77%	75%	100%	91%	59%	55%
4200	100%	92%	76%	74%	100%	91%	57%	53%
4400	100%	92%	75%	73%	100%	91%	55%	51%
4600	100%	91%	74%	72%	100%	90%	53%	49%
4800	100%	91%	73%	71%	100%	90%	51%	47%
5000	100%	91%	72%	70%	100%	89%	49%	45%
5200	100%	90%	71%	69%	100%	89%	47%	42%
5400	100%	90%	70%	68%	100%	89%	45%	40%
5600	100%	90%	70%	67%	100%	88%	43%	38%
5800	100%	89%	69%	66%	100%	88%	41%	36%
6000	100%	89%	68%	65%	100%	87%	39%	34%
6200	100%	89%	67%	64%	100%	87%	37%	32%
6400	100%	88%	66%	63%	100%	87%	35%	30%
6600	100%	88%	65%	62%	100%	86%	33%	27%
6800	100%	88%	65%	62%	100%	86%	31%	25%
7000	100%	87%	64%	61%	100%	85%	29%	23%
7200	100%	87%	63%	60%	100%	85%	27%	21%
7400	100%	87%	62%	59%	100%	85%	25%	19%
7600	100%	86%	62%	58%	100%	84%	23%	17%
7800	100%	86%	61%	57%	100%	84%	21%	14%

8000	100%	86%	60%	57%	100%	83%	19%	12%

The thermal aging is the battery degradation impacted by the battery operating temperature. For the thermal-aging rate (τ_a), the capacity loss dependence on temperature was modeled using an Arrhenius-like equation to fit the experimental data, so the aging degradation model is an empirical equation, as shown in Eqns. (10) and (11) [57].

$$\sigma_{fcn} = (\alpha \cdot SOC - \beta) \cdot \exp\left(\frac{-E_a + \eta \cdot I_c}{R_g \cdot (273.15 + T_b)}\right) \quad (10)$$

$$\tau_a = 1 - \sigma_{fcn} Q_{acc}{}^{\overline{z}} \quad (11)$$

Where, σ_{fcn} is the severity factor for the battery aging degradation; α, β, η and $\overline{z}$ are given parameters, obtained through fitting the experimental data. α=2897.8 and β=7413.1 when SOC<0.45; α=2694.3 and β=6025.6 when SOC≥0.45 [57]. R_g is the universal gas constant; E_a is the activation energy, equaling to 31,500 J/mol. I_c is the current rate of the battery (1/h). Q_{acc} is the cumulative capacity output of the battery throughout battery life so far (As). T_b is the battery's temperature (C). τ_a is the thermal-aging rate (% of battery initial capacity). The remaining battery capacity ($C_{bat,r}$, Ah) considering battery aging is calculated based on Eqn. (12).

$$C_{bat,r} = C_{bat,ini} \tau_a \tau_c \quad (12)$$

Where, $C_{bat,ini}$ is the initial battery capacity, Ah.

3.1.3. Battery electric-thermal module

The battery system, as the only energy source in BEV, provides energy for moving the vehicle (W_{pt}) and for working by BTMS (W_{btms}) and HVAC (W_{hvac}) system, and couples with the working of the RBS (W_{rbs}), as shown in Eqn. (13).

$$W_{bat} = W_{pt} + W_{hvac} + W_{btms} + W_{rbs} \quad (13)$$

Internally, the energy outflow/inflow of the battery system can be measured by Eqn. (14).

$$\frac{dW_{bat}}{dt} = P_{bat} = (OCV + I_c \cdot R_{bat}) \cdot I_c \quad (14)$$

Where, OCV is the open circuit voltage (V); I_c is the battery current (A); and R_{bat} is the battery internal resistance (Ω). The relation between battery SOC and battery current is given by Eqn. (15), a Coulomb counting method. The relation between battery generated heat and battery current is given by Eqn. (16).

$$\frac{dSOC}{dt} = I_c / C_{bat,r} \quad (15)$$

$$\frac{dQ_{bat}}{dt} = {I_c}^2 \cdot R_{bat} \quad (16)$$

Where, $C_{bat,r}$ is the battery rated capacity (Ah). Q_{bat} is the heat (J) generated from the battery system.

The other method to estimate the SOC is the voltage method, in which battery open circuit voltage (OCV) can be converted to equivalent SOC value using the battery's predefined discharge curve. The curve shown in Table 8 is used in this study.

Table 8. Relation between the SOC and OCV (V).

SOC	Open circuit voltage (V)
0.00	333
0.20	351
0.50	364
0.90	388
1.00	400

The battery's internal resistance (R_{bat}) is also impacted by the battery's electrochemical kinetics and temperature. Considering the complexity of the battery electrochemical kinetics, this study uses a similar interpolation and fitting function combined with the lookup table method, as described in Section 3.1.3, to determine the resistance value, as shown in Table 9.

Table 9. Relation between battery internal resistance with the SOC and temperature (°C).

Internal resistance (Ω)			
Battery temperature (°C) / SOC	**-15**	**0**	**30**
0.00	1.340	1.080	0.320
0.10	1.340	1.080	0.200
0.20	1.340	1.080	0.150
0.30	1.340	0.300	0.125
0.40	0.680	0.250	0.125
0.50	0.485	0.260	0.130
0.60	0.430	0.250	0.130
0.70	0.415	0.240	0.160
0.80	0.420	0.255	0.165
0.90	0.430	0.260	0.130
1.00	0.440	0.270	0.130

Because temperature is a significant factor determining the battery working status and lifetime [22], the BTMS is integrated in the BREVO model to adjust the temperature of the battery system for optimizing its working environment. There are two key parameters to determine how much energy transferred by and consumed by the BTMS: the temperature of battery (T_{bat}, °C), and the effective heat transfer coefficient between battery and BTMS (K_{btms},

W/K). When the temperature of battery is higher than the upper bound of the monitoring temperature ($T_{b,\,up}$, default value is set to 30 ℃), the BTMS will start to remove extra heat from the battery system. The amount of heat transfer will not change with temperature anymore when the temperature of battery is higher than 40 ℃ (the upper bound of the monitoring temperature + 10 ℃), as shown in Eqn. (17).

$$\frac{dQ_{btms}}{dt} = -K_{btms} \cdot min\left(T_{bat} - T_{b,up}, 10\right), where\ T_{bat} \geq T_{b,up} \quad (17)$$

Where, Q_{btms} is the heat added to or removed from the battery by the BTMS (J). When the temperature of battery is lower than the lower bound of the monitoring temperature ($T_{b,low}$, default value is set to 10 ℃), the BTMS will start to add extra heat and to increase the temperature of the battery system. The amount of heat transfer will not change with temperature anymore when the temperature of battery is lower than 0 ℃ (the lower bound of the monitoring temperature - 10 ℃).

$$\frac{dQ_{btms}}{dt} = K_{btms} \cdot min(T_{b,low} - T_{bat}, 10), where\ T_{bat} \leq T_{b,low} \quad (18)$$

Accordingly, the energy provided for the BTMS working is calculated through the efficiency f_{btms}.

The heat transfer from/to the battery system is not only with the BTMS, but also related to the ambient, the HVAC system. Eqns. (19-20) describe these heat transfer relationships.

$$C_{bat}\frac{dT_{bat}}{dt} = K_{ab}(T_a - T_{bat}) + K_{bc}(T_c - T_{bat}) + \frac{dQ_{btms}}{dt} + \frac{dQ_{bat}}{dt} \quad (19)$$

$$C_c \frac{dT_c}{dt} = K_{ac}(T_a - T_c) + K_{bc}(T_{bat} - T_c) + \frac{dQ_{rad}}{dt} + \frac{dQ_{hvac}}{dt} \quad (20)$$

Where, C_{bat} is heat capacity of battery (J/K); C_c is heat capacity of vehicle cabin (J/K); T_a is the temperature of ambient air (℃); T_{bat} is the temperature of battery (℃); T_c is the temperature of vehicle cabin (℃); ; Q_{hvac} is the heat added to or removed from the cabin by the HVAC system (J); Q_{rad} is the solar irradiance, which is set as 0, a default value.

3.1.4. Battery charging module

The battery charging process is similar to the battery discharge except for the direction of energy flow. During battery charging, the variations of the battery capacity and the battery temperature are considered by the battery electric-thermal module, and the battery aging impacted by the electrochemical reactions is also considered by the battery aging module. Because of the heat generated from the battery charging, the charger level, or more specifically, the charging power, impacts the energy transfer from/to the HVAC system and BTMS. However, unlike the battery discharge for moving the vehicle, the battery charging does not need to evaluate the regenerative energy from the RBS. Since the BREVO model has a driving profile, it can filter and count the locations where the vehicle stops for longer than 10 minutes, which are regarded to be potential for charging. This paper assumes that the driver's home is available for charging when the battery SOC is less than 0.2.

3.2. The driver-end features in the BREVO model

The driver-end features in the BREVO model provide the yearly second-by-second driving profile for simulating the vehicle powertrain and battery lifetime under real-world

driving conditions. Thus, the daily/monthly trips, the driving cycles in a specific trip, and the local temperatures during the specific trips are all created by the BREVO model. Figure 2 presents the logic flow to create the real-world second-by-second driving profile in the BREVO model. Based on the National Household Travel Survey (NHTS) trip information [59], driving profiles for each trip, and the corresponding local ambient temperature data, we can create a year-round driving profile for a random driver in a specific location in the U.S. For simplification, we assume the driving profile in other years repeats the driving profile for the first year, so this study can simulate the real-world driving patterns for BEV in the BREVO model. The pseudo-driving profile also provides effective information on the trip destinations and dwell times, so the BREVO can be used for optimizing the charging based on driver patterns.

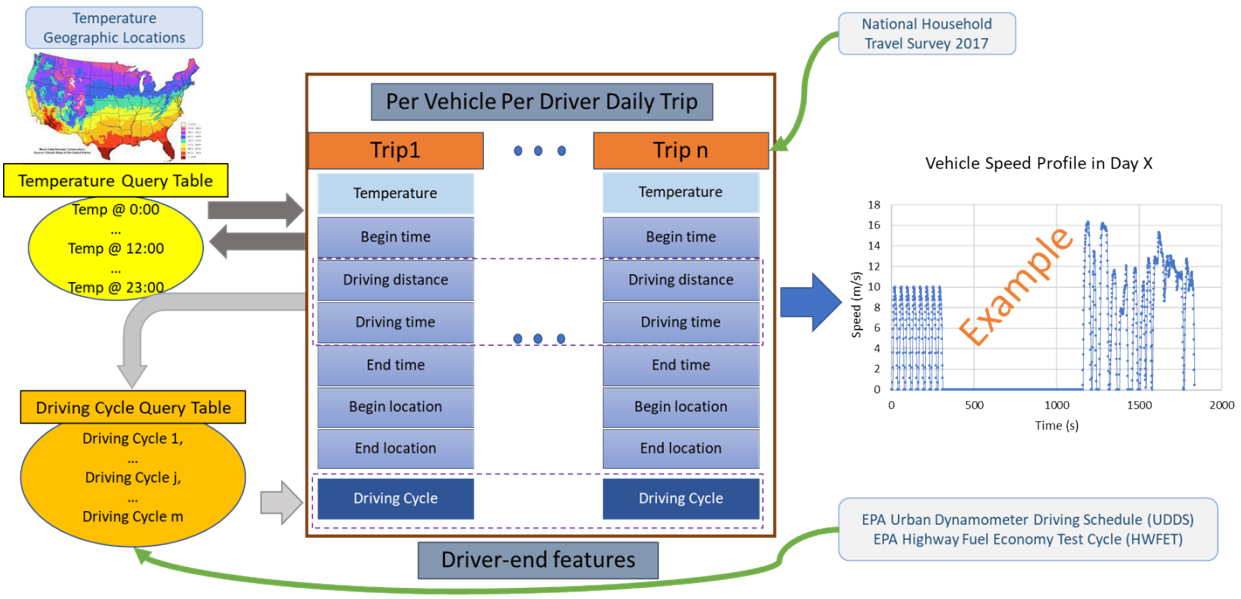

Figure 2. Driver-end features of BREVO model.

To begin with the creation of the yearly second-by-second driving profile for vehicle drivers, this study uses the trip information from the NHTS as the driver patterns for simulation.

The trip includes the daily travel information for a whole year from different drivers and locations in the U.S. Each trip includes information such as begin time, driving distance, driving time, end time, begin location, and end location. Based on the trip information, the driving average speed and driving purpose in each trip is also obtained. All the trip information provides the skeleton of the travel patterns for each day in a year. The study randomly picks the trip information to make up a random driver's yearly trip information in a specific location.

The Urban Dynamometer Driving Schedules (UDDS), and the Highway Fuel Economy Test Cycle (HWFET) are regarded to be the most common driving cycles for U.S. private drivers and are often used for vehicle and fuel emissions testing by the U.S. Environmental Protection Agency (EPA). To create the second-by-second vehicle speed profile, this study cuts the driving cycles into several slices and puts them in a driving profile pool. The slice numbers can be customized by the BREVO model: in this paper, two slices of the HWFET driving cycles and four slices of the UDDS driving cycles are created. Based on the criterion – trip average speed and trip driving time that we obtain from the NHTS trips, the BREVO model automatically generates a new second-by-second driving cycle profile for specific trips by matching and connecting the driving cycle slices from the driving profile pool.

In addition, this study matches the atmospheric temperature data, collected from the National Oceanic and Atmospheric Administration (https://www.ncdc.noaa.gov/cdo-web/datasets), with the trip driving profiles based on the trip beginning time, trip end time, and trip locations. The atmospheric temperature will work as the ambient temperature for the BEV

simulation in the BREVO model. The atmospheric temperature is collected hourly, so this study assumes the ambient temperature within the same hour does not change.

3.3. The use of BREVO model

Implemented and coded using Microsoft Excel® for Windows and Visual Basic Analysis (VBA), the BREVO simulates the impacts of different vehicle-, battery- and driver- features on long-term battery capacity evolution. Considering the vehicle-, battery- and driver- features vary, this study releases the BREV model on GitHub (https://github.com/ous-ornl/brevo), which will be convenient for the public to use and to customize the features, such as the powertrain metrics, the battery experimental data, and the driver travel patterns. The main interface of the BREVO model is shown in Figure 3. The users can change the values in the *Initial Inputs* box and the *Charging* box, such as temperature and simulation time step; also, the users can set up the *HVAC*, *BTMS*, *RBS*, and *Charger Type* based on the scenarios needed. In the *Results* box, the users can see the summarized information when the simulation is done, more detailed results for each day can be found in the worksheet tab - *Results*. When beginning the simulation, the user needs to click the button – *Trip Simulation*, and then select all the daily trip files (.xls or .xlsx format). The BREVO model will start to run till the end. The user can click the button – *Reset to Default* for resetting the model. The defaulted daily trip files for the New England area have been uploaded to GitHub as well for users to test. The user should extract all daily trip zip files (*Boston_DayTrips_Part1.zip* to *Boston_DayTrips_Part1.zip*) into one folder before selecting these daily trip files.

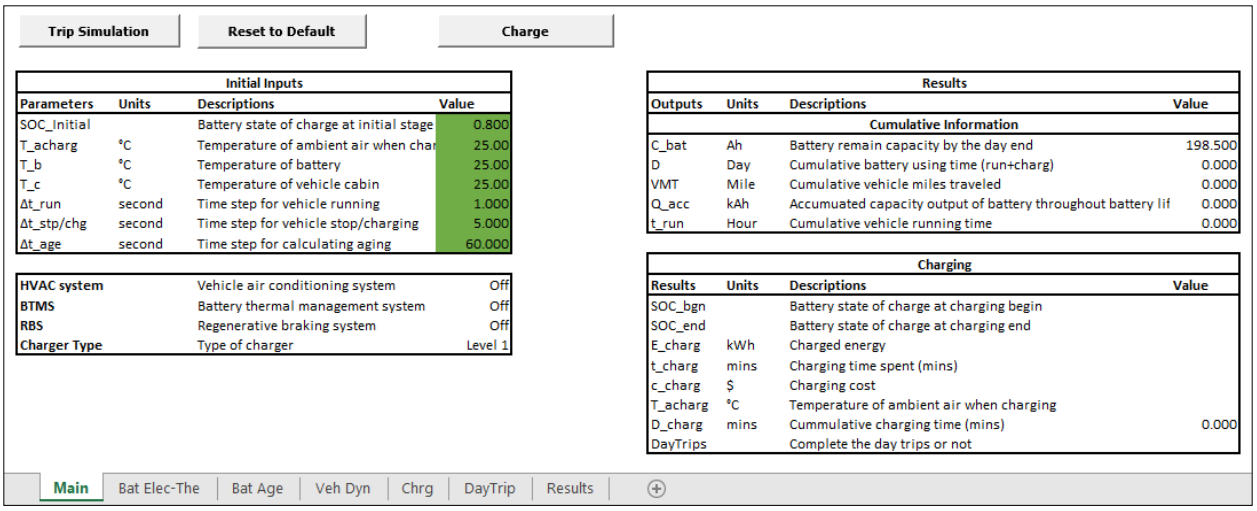

Figure 3. The main interface of the BREVO model.

In addition to the Main tab, the BREVO model allows the user to customize the battery-related settings, vehicle and powertrain metrics, and driver travel patterns based on their demands. The tab – *Bat Elec-The* includes battery general information, heat transfer, and thermal management system information; in addition, the user can revise the metrics shown in Table 8 and Table 9 based on their real experimental results. The model will automatically look up the table, quickly build up the fitting equations, and calculate the results through the interpolation of the fitting equations. Similarly, the users can change the battery aging information in the Excel tab – *Bat Age*, vehicle information in the Excel tab – *Veh Dyn*, and charging information in the Excel tab – *Chrg*. The Excel tab – *DayTrip* is used for generating daily pseudo-second-by-second driving cycles if the users have only trip information, for example, the NHTS information. For creating the pseudo, the users should first input the trip information following the format shown in the tab – *DayTrip*, then click the button – *Trip Generator*, and the users will need to select all the driving cycles Excel files, which can be downloaded and unzipped from the GitHub (*DrivingCycles.rar*). The last Excel tab – *Results* will show all daily simulation results including information on battery, vehicle, and travel patterns.

4. Results and Discussions

4.1. DC fast charging could cause up to 22% less battery capacity than L1 charging

To compare the impacts of different charging levels on battery aging, this study creates the yearly second-by-second driving profile of a random driver from New England. The travel patterns and trip features of this random driver are shown in Figure 4. In summary, the annual travel mileage of this random driver is about 13,234 miles, and a total of 1374 trips are driven in a year. The distance of over 95% of these trips is less than 30 miles, and the travel time of over 81% of these trips is less than 30 mins. The driver's most frequent destinations are areas in Massachusetts, Vermont, New Hampshire, Connecticut, and Rhode Island. Therefore, the BEV with a battery size of 198.5 Ah can meet most daily trips of this random driver. In fact, this study assumes the driver uses overnight charging only unless the driver cannot complete the trip in a specific day; and the model results show that the overnight charging method fails to meet the travel demands of two days only in a year.

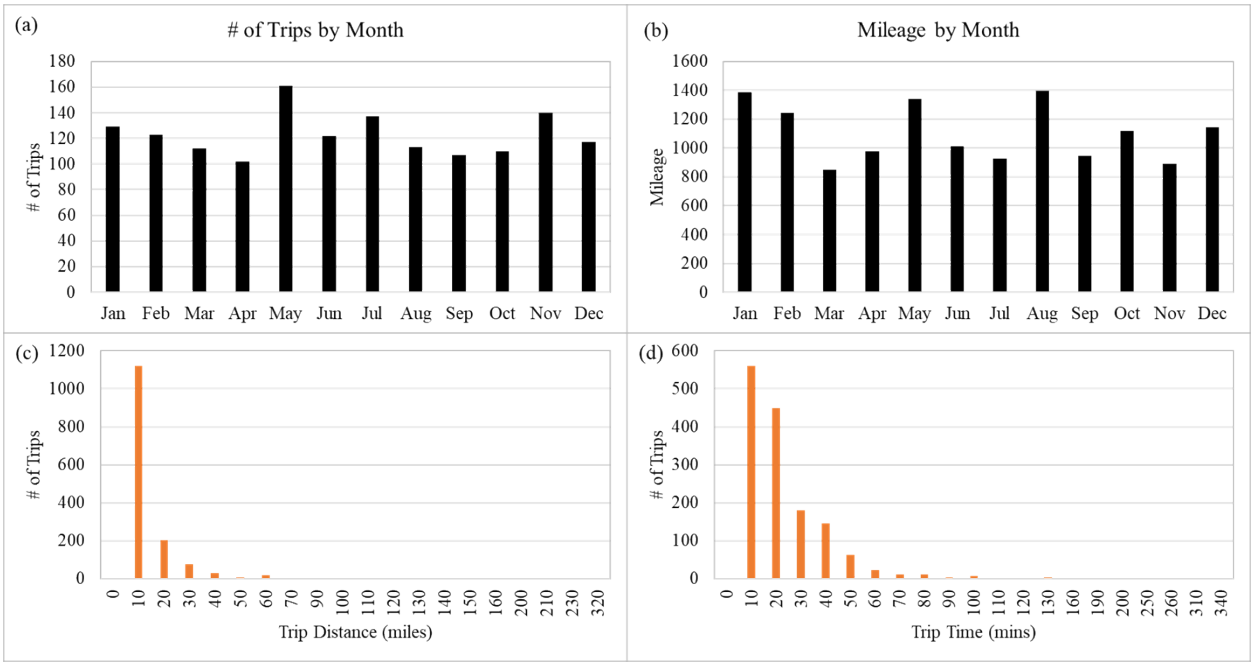

Figure 4. The travel patterns of a random driver in New England.

Based on the driving profile described above, this study uses the BREVO to compare the BEV usage by charging with the Level 1 (L1) charger and the DC FC respectively to quantify the impacts of charging level. For the L1 charger, the charging power is 1.8 kW, the maximum charging voltage is 120 V, and the charging efficiency is 85%. For the DC FC, the charging power is 60 kW, the maximum charging voltage is 480 V, and the charging efficiency is 85%. In addition, the model assumes that the drivers will not charge the car if the available battery energy is enough to complete the trips the next day.

The BREVO model calculates the remaining battery capacity levels, and the results are presented in Figure 5. The initial battery capacity of the BEV is 198.5 Ah, equaling 100% battery capacity percentage when the simulation starts. Clearly, the battery's state of health fades as a function of time, and the charging method also impacts the battery's aging speed. By the end of the 10th year, the average remaining battery capacity reaches 86% of the initial battery capacity

by using the L1 charger as the only overnight charging method; the remaining battery capacity reaches 67% of the initial battery capacity by using DC FC as the only overnight charging method. The average battery remaining capacity after using the DC FC for ten years as the only overnight charging method is up to 22% lower than it is after using the L1 charger. In addition, Figure 5(b) gives the remaining battery capacity along with the driving mileage by every 1000 miles. It shows the general trend of the remaining battery capacity decreasing, and the waves show the seasonable (temperature) impacts on the remaining battery capacity.

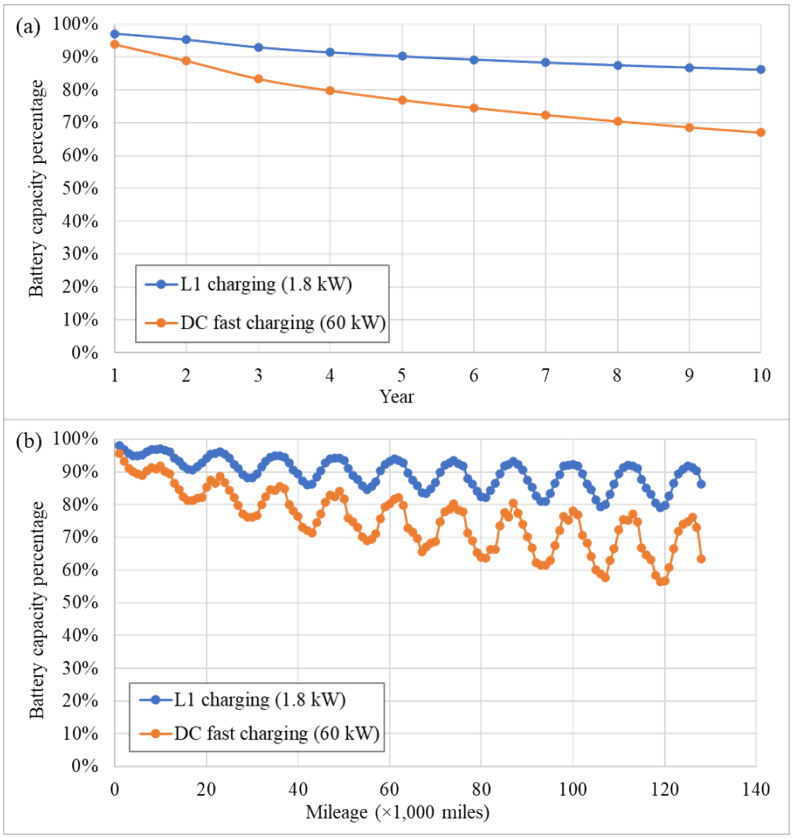

Figure 5. (a) The remaining battery capacity (by percentage) by year; and (b) the remaining battery capacity (by percentage) by mileage.

4.2. BTMS favors the battery lifetime

The BREVO model integrates the HVAC system, RBS, and BTMS so it can quantify the performance of these subsystems for prolonging the lifetime of the BEV's battery. Figure 6 shows the comparisons of the relative remaining battery capacity after one year of driving profile simulation under different scenarios. The benchmarking is the scenario where the BEV runs on the driving profile with HVAC off, RBS off, and BTMS off. The BTMS_On is the scenario where the BEV runs on the driving profile with only BTMS on. The HVAC_On is the scenario where the BEV runs on the driving profile with only the HVAC system on. The RBS_On is the scenario where the BEV runs on the driving profile with only RBS on. Clearly, the results show that BTMS is beneficial in delaying battery degradation in the BEV. The remaining battery capacity with the BTMS improves by 0.5% relative to the benchmark; however, the use of the HVAC system can speed up the battery degradation. The RBS does not have remarkable impacts on the remaining battery capacity. Noticeably, the driving profile used for the simulation is the same as the one in the previous section, which is the driving profile for a random driver in the New England area. Therefore, the impacts of these subsystems (BTMS, HVAC system, and RBS) could vary under different locations or travel patterns. In addition, the simulation is only for one-year impacts, so longer impacts on battery degradation still need more research.

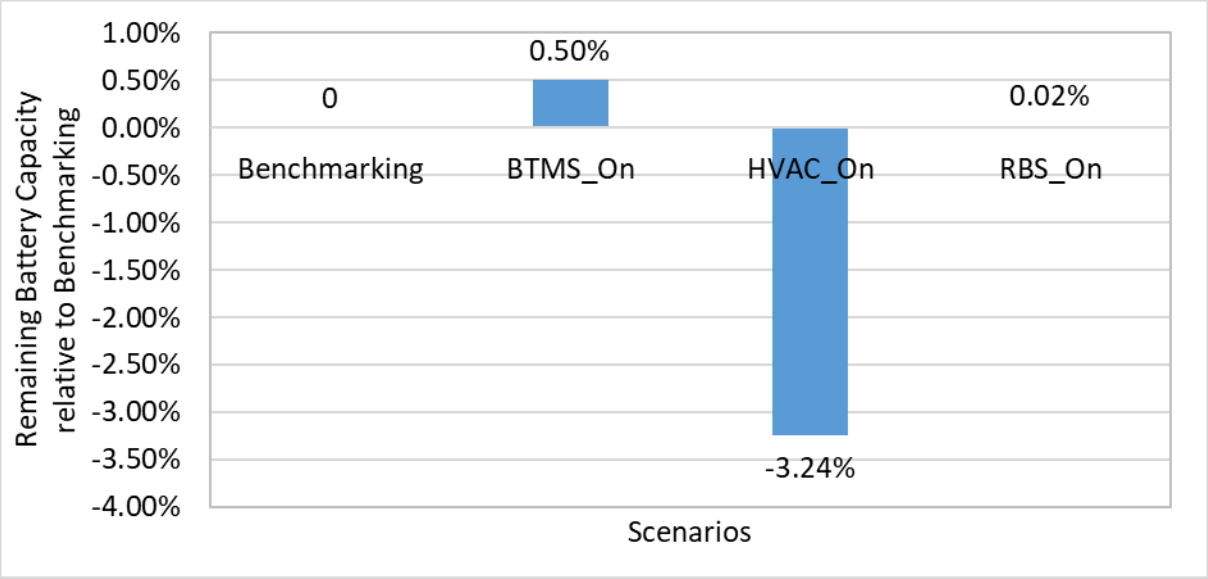

Figure 6. Remaining battery capacity (%) relative to the Benchmarking scenario.

4.3. Ambient temperature impacts the battery lifetime

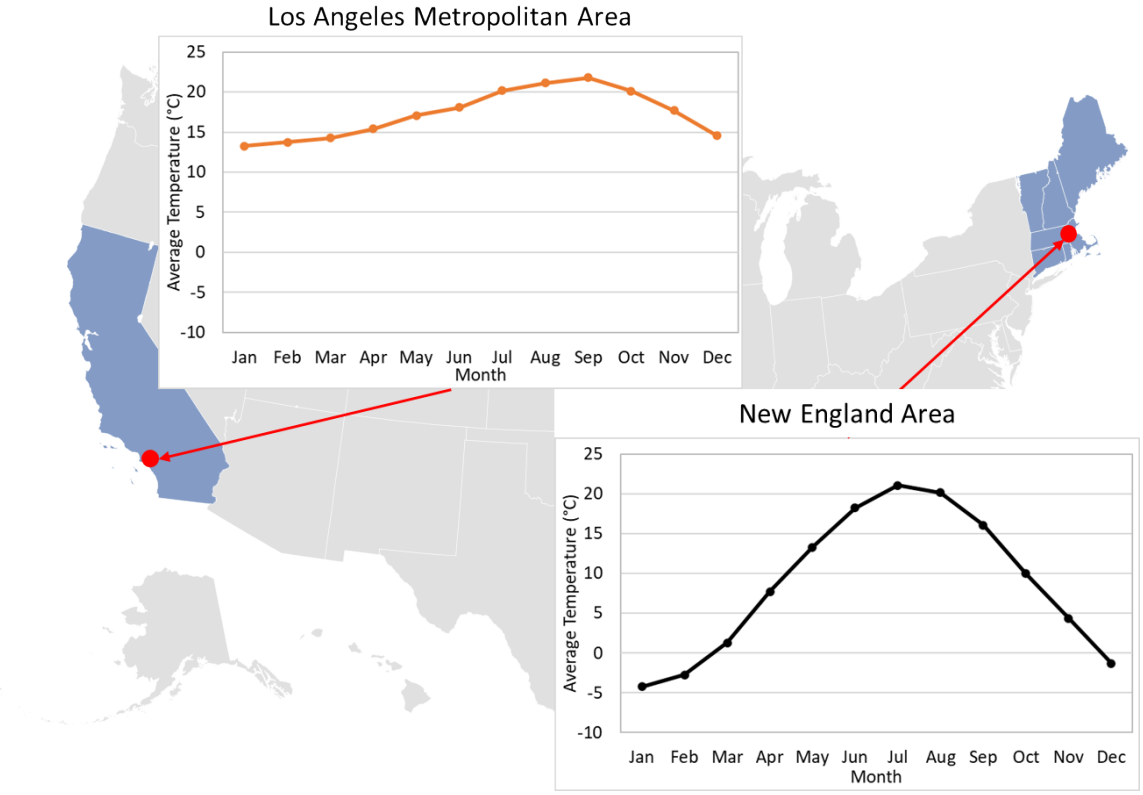

Figure 7. The average temperature in the New England area (including Boston metropolitan area) and in the Los Angeles metropolitan area, respectively [60].

The temperature is a critical factor to determine the battery usage for a BEV. As shown in Eqn. (15-16), the ambient temperature changes the working temperature of the battery if no BTMS is used for adjustment, and the battery working temperature can determine the battery efficiency (by impacting the battery's internal resistance) and the battery aging rate as well. Figure 7 presents the yearly temperatures from the New England area (including Boston metropolitan area) and the Los Angeles Metropolitan area respectively [60]. As shown in Figure 8, the temperature trends vary substantially: the average temperature in the New England area changes from -4 °C in January to 21 °C in July; while the average temperature in the Los Angeles Metropolitan area changes from 13 °C in January to 22 °C in August. Los Angeles provides a more temperature-friendly environment for the BEV battery than the New England area. To understand the impact of temperature on the vehicle battery lifetime, the BREVO model controls simulations with the same BEV, the same random driver with the same travel patterns, but with different temperature trend profiles: the New England area temperature; and the Los Angeles temperature. The simulation results are shown in Figure 8. After the simulation for a one-year driving profile, the remaining battery capacity in the New England area drops to no more than 92%, and the remaining battery capacity in the Los Angeles metropolitan area drops to no more than 95%. As the battery continues usage in these two areas in the following years, the differences caused by temperature could be even larger. In the 10^{th} year, the remaining battery capacity in the New England area is about 81%, and the remaining battery capacity in the Los Angeles metropolitan area drops to no more than 86%. It shows that the ambient temperature could cause different health statuses of the battery: the BEV's battery capacity is 6% more in the Los Angeles area than in the New England area after 10-year use when the driver patterns and vehicle are the same.

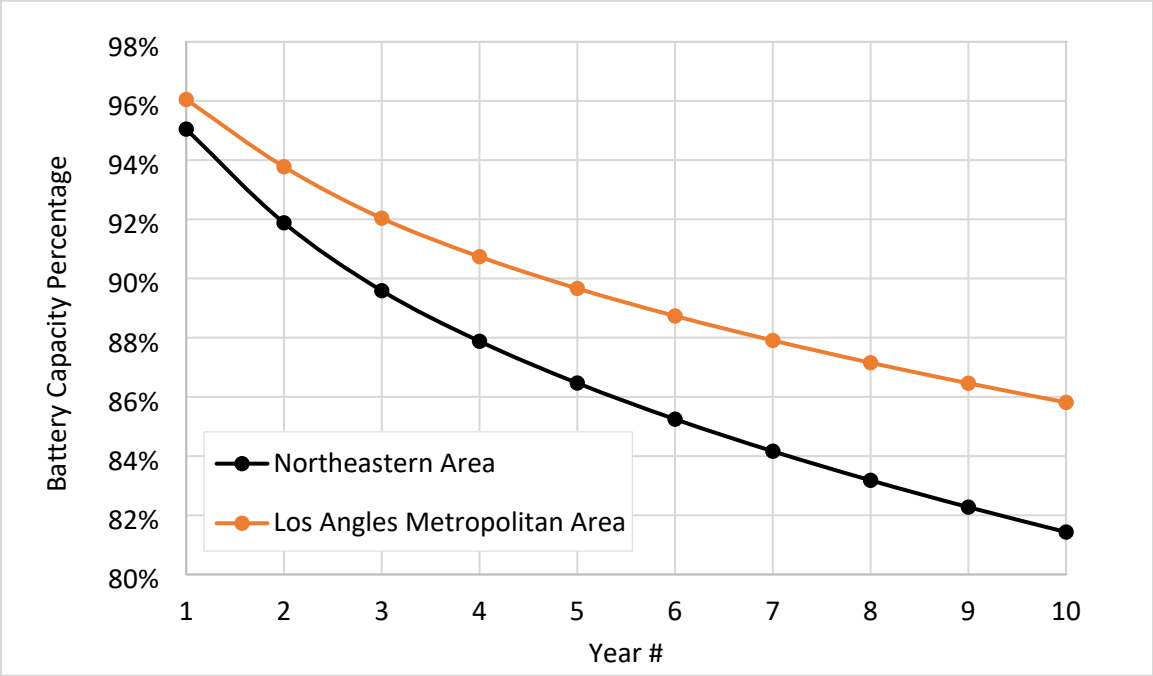

Figure 8. Remaining battery capacity (%) by week in a calendar year.

5. Conclusions

This study presents the development of the BREVO model, which takes into account both the vehicle-end features and the driver-end features related to BEV use. The model constructs real-world driving profiles for the BEV powertrain, with a particular focus on battery simulations. Additionally, this study reviews potential end-use factors that could cause battery degradation and reduce battery lifetime, including driving patterns, charging behavior, terrain, ambient temperature, charging power, and calendar degradation. It aims to quantify the battery degradation impacted by charging and driver's travel patterns and provide insights to inform stakeholders involved in BEV battery design and the electric vehicle market.

This study reveals that the DC FC, while beneficial to BEV users by saving time, can cause battery degradation, resulting in a maximum of 22% less battery capacity compared to daily Level-1 charging for a random driver located in the New England area after ten years of use. The BTMS can help to delay battery degradation by about 0.5% compared to a BEV without the BTMS after simulation with a one-year driving profile in the New England area. The ambient temperature also impacts BEV battery degradation, as the simulation example shows that a warmer temperature, such as that in the Los Angeles metropolitan area, allows the BEV to remain at a higher battery capacity level for driver usage than when used in the New England area.

The study's contributions lie in creating a modeling framework for investigating the impacts of vehicle-end features and driver-end factors on BEV battery degradation and its coupling with the whole BEV powertrain system. However, this study at the current stage still has some caveats and limitations that need much effort to improve in the future.

- First of all, the premise of the analysis is that the battery is lithium-ion material, and the battery experiment test data are collected through the publications. The test data for battery and the vehicle powertrain features and design parameters vary for different BEVs, and they should be updated for different vehicle models or battery designs.
- Secondly, the relation between the DoD and the discharge cycles, as shown in Table 3, is simplified with a fitting equation. However, from a battery pack perspective, the discharging cycle numbers depend on not only the chemistry but also other factors such as the battery design and the testing protocols.

- The experimental data for specific battery types and BEV types are needed for improving the simulation accuracy. For example, the thermal model discussed in Section 3.1.3 presumed that an average temperature of the battery system applies to all battery cells; However, this simplifies the complexity of the battery system since a high-temperature gradient exists within the battery [61]. The analysis and model will be updated and improved, as more real-world data becomes available from BEV drivers and manufacturers.
- In the next phase of the BREVO model, it will integrate with reinforcement learning to help the consumer to optimize the decisions on charging (charging rate, charging time, and charging capacity needed) based on the objection function which considers both the long-term goal – an extension of battery remaining capacity, and the short-term goal – relief the electric range anxiety.

At last, the BREVO model and relative supported files can be downloaded on GitHub (https://github.com/ous-ornl/brevo). The password for access to the code in VBA of the BREVO model is available from the author upon request. A new version of the model will be released based on external and internal feedback as well.

6. Acknowledgments

The author thanks the funding support of the Department of Energy's Vehicle Technology Office. The author is grateful to Jake Herb of the Department of Energy, Jianlin Li and Burak Ozpineci of the Oak Ridge National Laboratory whose suggestions and comments have greatly improved the clarity of the paper. The views and opinions of the author expressed herein do not necessarily state or reflect those of the United States Government or any agency thereof. Neither the United States Government nor any agency thereof, nor any of their

employees, makes any warranty, expressed or implied, or assumes any legal liability or responsibility for the accuracy, completeness, or usefulness of any information, apparatus, product, or process disclosed, or represents that its use would not infringe privately owned rights.

7. Author Contributions

Shiqi Ou: Conceptualization, Methodology, Software, Visualization, Investigation, Data curation, Project administration, Supervision, Funding acquisition, Formal analysis, Resources, Validation, Writing - original draft, Writing - review & editing.

8. References

[1] S. Ou, D. Gohlke, Z. Lin, Quantifying the impacts of micro- and mild- hybrid vehicle technologies on fleetwide fuel economy and electrification, ETransportation. 4 (2020) 100058. doi:https://doi.org/10.1016/j.etran.2020.100058.

[2] L. Paoli, T. Gül, Electric cars fend off supply challenges to more than double global sales, Int. Energy Agency. (2022). https://www.iea.org/commentaries/electric-cars-fend-off-supply-challenges-to-more-than-double-global-sales (accessed May 5, 2022).

[3] IEA, Global EV Outlook 2020, Paris, France, 2020. https://www.iea.org/reports/global-ev-outlook-2020.

[4] White House, FACT SHEET: President Biden Sets 2030 Greenhouse Gas Pollution Reduction Target Aimed at Creating Good-Paying Union Jobs and Securing U.S. Leadership on Clean Energy Technologies, White House Brief. Room. (2021). https://www.whitehouse.gov/briefing-room/statements-releases/2021/04/22/fact-sheet-president-biden-sets-2030-greenhouse-gas-pollution-reduction-target-aimed-at-creating-good-paying-union-jobs-and-securing-u-s-leadership-on-clean-energy-technologies/ (accessed March 14, 2022).

[5] U.S. Department of State, U.S. Executive Office of the President, The Long-Term Strategy of the United States: Pathways to Net-Zero Greenhouse Gas Emissions by 2050, Washington, DC, 2021. https://www.whitehouse.gov/wp-content/uploads/2021/10/US-Long-Term-Strategy.pdf.

[6] Volvo Global Newsroom, The Future is Electric, Volvo Glob. Newsroom. (2020). https://group.volvocars.com/company/innovation/electrification (accessed August 3, 2022).

[7] P.A. Eisenstein, Detroit's Big Three automakers are looking to a battery-powered future, but each is forging its own path, CNBC. (2019). https://www.cnbc.com/2019/12/08/us-automakers-look-to-a-battery-powered-future-but-forge-their-own-paths.html (accessed August 3, 2022).

[8] T. Moss, Chinese Cars Are Still Cheap, But They're No Longer Ugly, Wall Str. J. (2019). https://www.wsj.com/articles/chinese-cars-are-still-cheap-but-theyre-no-longer-ugly-11548417621 (accessed January 12, 2020).

[9] J. Whalen, The next China trade battle could be over electric cars, Washington Post. (2020). https://www.washingtonpost.com/business/2020/01/16/next-china-trade-battle-could-be-over-electric-cars/ (accessed July 6, 2020).

[10] DOE Office of Technology Transitions, Solving Challenges in Energy Storage, Washington, D.C., 2018. https://www.energy.gov/sites/prod/files/2018/09/f55/2018-08-23_Spotlight on Energy Storage - Brochure and Success Stories_0.pdf.

[11] Vehicle Technologies Office, FOTW #1272, January 9, 2023: Electric Vehicle Battery Pack Costs in 2022 Are Nearly 90% Lower than in 2008, according to DOE Estimates, U.S. Dep. Energy. (2023). https://www.energy.gov/eere/vehicles/articles/fotw-1272-january-9-2023-electric-vehicle-battery-pack-costs-2022-are-nearly (accessed March 22, 2023).

[12] K. Turcheniuk, D. Bondarev, V. Singhal, G. Yushin, Ten years left to redesign lithium-ion batteries, Nature. 559 (2018). doi:10.1038/d41586-018-05752-3.

[13] Transportation Research Board, National Research Council, Charging Infrastructure for Plug-in Electric Vehicles, in: Overcoming Barriers to Deploy. Plug-in Electr. Veh., The National Academies Press, Washington, D.C., 2015. doi:10.17226/21725.

[14] U.S. Department of Energy, President Biden, DOE and DOT Announce $5 Billion over Five Years for National EV Charging Network, U.S. Dep. Energy. (2022). https://www.energy.gov/articles/president-biden-doe-and-dot-announce-5-billion-over-five-years-national-ev-charging (accessed August 4, 2022).

[15] S. Ou, Z. Lin, X. He, S. Przesmitzki, J. Bouchard, Modeling charging infrastructure impact on the electric vehicle market in China, Transp. Res. Part D Transp. Environ. 81 (2020) 102248. doi:https://doi.org/10.1016/j.trd.2020.102248.

[16] DOE, Developing Infrastructure to Charge Electric Vehicles, Altern. Fuels Data Cent. (2023). https://afdc.energy.gov/fuels/electricity_infrastructure.html (accessed May 4, 2020).

[17] J.A. Domínguez-Navarro, R. Dufo-López, J.M. Yusta-Loyo, J.S. Artal-Sevil, J.L. Bernal-Agustín, Design of an electric vehicle fast-charging station with integration of renewable energy and storage systems, Int. J. Electr. Power Energy Syst. 105 (2019) 46–58. doi:10.1016/j.ijepes.2018.08.001.

[18] Y. Xiong, J. Gan, B. An, C. Miao, A.L.C. Bazzan, Optimal Electric Vehicle Fast Charging Station Placement Based on Game Theoretical Framework, IEEE Trans. Intell. Transp. Syst. 19 (2018) 2493–2504. doi:10.1109/TITS.2017.2754382.

[19] U.S. Department of Energy, Enabling Fast Charging: A Technology Gap Assessment, Washington, D.C., 2017. doi:10.2172/1466683.

[20] N. Omar, M.A. Monem, Y. Firouz, J. Salminen, J. Smekens, O. Hegazy, H. Gaulous, G. Mulder, P. Van den Bossche, T. Coosemans, J. Van Mierlo, Lithium iron phosphate based battery – Assessment of the aging parameters and development of cycle life model, Appl. Energy. 113 (2014) 1575–1585. doi:10.1016/j.apenergy.2013.09.003.

[21] S.S. Sebastian, B. Dong, T. Zerrin, P.A. Pena, A.S. Akhavi, Y. Li, C.S. Ozkan, M. Ozkan, Adaptive fast charging methodology for commercial Li-ion batteries based on the internal resistance spectrum, Energy Storage. n/a (2020) e141. doi:10.1002/est2.141.

[22] J. Neubauer, Battery lifetime analysis and simulation tool (BLAST) documentation, National Renewable Energy Lab.(NREL), Golden, CO (United States), Golden, CO, 2014. https://www.nrel.gov/docs/fy15osti/63246.pdf.

[23] X. Han, L. Lu, Y. Zheng, X. Feng, Z. Li, J. Li, M. Ouyang, A review on the key issues of the lithium ion battery degradation among the whole life cycle, ETransportation. 1 (2019) 100005. doi:10.1016/j.etran.2019.100005.

[24] Hearst Autos Research, Electric Car Battery Life: Everything You Need to Know, Car Driv. (2020). https://www.caranddriver.com/research/a31875141/electric-car-battery-life (accessed August 3, 2022).

[25] Tesloop, Tesloop's Tesla Model S Surpasses 400,000 Miles, Tesloop.Com. (2018). https://www.tesloop.com/blog/2018/7/16/tesloops-tesla-model-s-surpasses-400000-miles-643737-kilometers (accessed August 3, 2022).

[26] X. Hu, L. Xu, X. Lin, M. Pecht, Battery Lifetime Prognostics, Joule. 4 (2020) 310–346. doi:10.1016/j.joule.2019.11.018.

[27] A.A. Hussein, Experimental modeling and analysis of lithium-ion battery temperature dependence, in: 2015 IEEE Appl. Power Electron. Conf. Expo., 2015: pp. 1084–1088. doi:10.1109/APEC.2015.7104483.

[28] F. Leng, C.M. Tan, M. Pecht, Effect of Temperature on the Aging Rate of Li Ion Battery Operating above Room Temperature, Sci. Rep. 5 (2015) 12967. doi:10.1038/srep12967.

[29] T. Kern, P. Dossow, E. Morlock, Revenue opportunities by integrating combined vehicle-

to-home and vehicle-to-grid applications in smart homes, Appl. Energy. 307 (2022) 118187. doi:https://doi.org/10.1016/j.apenergy.2021.118187.

[30] Y. Al-Wreikat, C. Serrano, J.R. Sodré, Effects of ambient temperature and trip characteristics on the energy consumption of an electric vehicle, Energy. 238 (2022) 122028. doi:https://doi.org/10.1016/j.energy.2021.122028.

[31] A.G. Mohammed, K.E. Elfeky, Q. Wang, Recent advancement and enhanced battery performance using phase change materials based hybrid battery thermal management for electric vehicles, Renew. Sustain. Energy Rev. 154 (2022) 111759. doi:https://doi.org/10.1016/j.rser.2021.111759.

[32] J. Zhao, H. Ling, J. Liu, J. Wang, A.F. Burke, Y. Lian, Machine learning for predicting battery capacity for electric vehicles, ETransportation. 15 (2023) 100214. doi:https://doi.org/10.1016/j.etran.2022.100214.

[33] M. Jafari, A. Gauchia, S. Zhao, K. Zhang, L. Gauchia, Electric Vehicle Battery Cycle Aging Evaluation in Real-World Daily Driving and Vehicle-to-Grid Services, IEEE Trans. Transp. Electrif. 4 (2018) 122–134. doi:10.1109/TTE.2017.2764320.

[34] K.A. Severson, P.M. Attia, N. Jin, N. Perkins, B. Jiang, Z. Yang, M.H. Chen, M. Aykol, P.K. Herring, D. Fraggedakis, M.Z. Bazant, S.J. Harris, W.C. Chueh, R.D. Braatz, Data-driven prediction of battery cycle life before capacity degradation, Nat. Energy. 4 (2019) 383–391. doi:10.1038/s41560-019-0356-8.

[35] W. Gu, Z. Sun, X. Wei, H. Dai, A Capacity Fading Model of Lithium-Ion Battery Cycle Life Based on the Kinetics of Side Reactions for Electric Vehicle Applications, Electrochim. Acta. 133 (2014) 107–116. doi:https://doi.org/10.1016/j.electacta.2014.03.186.

[36] J. Henschel, F. Horsthemke, Y.P. Stenzel, M. Evertz, S. Girod, C. Lürenbaum, K. Kösters, S. Wiemers-Meyer, M. Winter, S. Nowak, Lithium ion battery electrolyte degradation of field-tested electric vehicle battery cells – A comprehensive analytical study, J. Power Sources. 447 (2020) 227370. doi:https://doi.org/10.1016/j.jpowsour.2019.227370.

[37] A. Millner, Modeling Lithium Ion battery degradation in electric vehicles, in: 2010 IEEE Conf. Innov. Technol. an Effic. Reliab. Electr. Supply, 2010: pp. 349–356. doi:10.1109/CITRES.2010.5619782.

[38] S. Saxena, C. Le Floch, J. MacDonald, S. Moura, Quantifying EV battery end-of-life through analysis of travel needs with vehicle powertrain models, J. Power Sources. 282 (2015) 265–276. doi:https://doi.org/10.1016/j.jpowsour.2015.01.072.

[39] M. Ecker, N. Nieto, S. Käbitz, J. Schmalstieg, H. Blanke, A. Warnecke, D.U. Sauer, Calendar and cycle life study of Li(NiMnCo)O2-based 18650 lithium-ion batteries, J. Power Sources. 248 (2014) 839–851. doi:https://doi.org/10.1016/j.jpowsour.2013.09.143.

[40] G. Ning, B.N. Popov, Cycle Life Modeling of Lithium-Ion Batteries, J. Electrochem. Soc. . 151 (2004) A1584–A1591. doi:10.1149/1.1787631.

[41] O. Gross, S. Clark, Optimizing Electric Vehicle Battery Life through Battery Thermal Management, SAE Int. J. Engines. 4 (2011) 1928–1943. http://www.jstor.org/stable/26278270.

[42] Battery University Group, BU-808: How to Prolong Lithium-based Batteries, Batter. Univ. Gr. (2021). https://batteryuniversity.com/learn/article/how_to_prolong_lithium_based_batteries (accessed July 27, 2022).

[43] E.D. Kostopoulos, G.C. Spyropoulos, J.K. Kaldellis, Real-world study for the optimal

charging of electric vehicles, Energy Reports. 6 (2020) 418–426. doi:https://doi.org/10.1016/j.egyr.2019.12.008.

[44] P. Mohtat, S. Lee, J.B. Siegel, A.G. Stefanopoulou, Comparison of expansion and voltage differential indicators for battery capacity fade, J. Power Sources. 518 (2022) 230714. doi:https://doi.org/10.1016/j.jpowsour.2021.230714.

[45] S.C. Davis, R.G. Boundy, Transportation Energy Data Book, Edition 39, Oak Ridge National Laboratory, TN (US), Oak Ridge, TN, USA, 2021. doi:10.2172/1767864.

[46] S. Ou, R. Yu, Z. Lin, H. Ren, X. He, S. Przesmitzki, J. Bouchard, Intensity and daily pattern of passenger vehicle use by region and class in China: estimation and implications for energy use and electrification, Mitig. Adapt. Strateg. Glob. Chang. (2019). doi:10.1007/s11027-019-09887-0.

[47] S. Xie, X. Hu, Q. Zhang, X. Lin, B. Mu, H. Ji, Aging-aware co-optimization of battery size, depth of discharge, and energy management for plug-in hybrid electric vehicles, J. Power Sources. 450 (2020) 227638. doi:https://doi.org/10.1016/j.jpowsour.2019.227638.

[48] L.-L. Lu, Y.-Y. Lu, Z.-X. Zhu, J.-X. Shao, H.-B. Yao, S. Wang, T.-W. Zhang, Y. Ni, X.-X. Wang, S.-H. Yu, Extremely fast-charging lithium ion battery enabled by dual-gradient structure design, Sci. Adv. 8 (2023) eabm6624. doi:10.1126/sciadv.abm6624.

[49] Z. Yang, J.W. Morrissette, Q. Meisner, S.-B. Son, S.E. Trask, Y. Tsai, S. Lopykinski, S. Naik, I. Bloom, Extreme Fast-Charging of Lithium-Ion Cells: Effect on Anode and Electrolyte, Energy Technol. 9 (2021) 2000696. doi:https://doi.org/10.1002/ente.202000696.

[50] P. Paulraj, Electric Vehicle Charging Levels, Modes and Types Explained | North America Vs. Europe Charging cables and plug types, E-Mobility Simpl. (2019).

https://www.emobilitysimplified.com/2019/10/ev-charging-levels-modes-types-explained.html (accessed July 28, 2020).

[51] Tesla, Supercharging, (2020). https://www.tesla.com/support/supercharging (accessed July 28, 2020).

[52] W. Xie, X. Liu, R. He, Y. Li, X. Gao, X. Li, Z. Peng, S. Feng, X. Feng, S. Yang, Challenges and opportunities toward fast-charging of lithium-ion batteries, J. Energy Storage. 32 (2020) 101837. doi:10.1016/j.est.2020.101837.

[53] L.-H. Björnsson, S. Karlsson, The potential for brake energy regeneration under Swedish conditions, Appl. Energy. 168 (2016) 75–84. doi:https://doi.org/10.1016/j.apenergy.2016.01.051.

[54] J. Neubauer, E. Wood, The impact of range anxiety and home, workplace, and public charging infrastructure on simulated battery electric vehicle lifetime utility, J. Power Sources. 257 (2014) 12–20. doi:https://doi.org/10.1016/j.jpowsour.2014.01.075.

[55] C.W. Maranville, J. Schneider, L. Chaney, T. Barnh, J.P. Heremans, Improving efficiency of a vehicle HVAC system with comfort modeling, zonal design, and thermoelectric devices, in: DEER Conf., U.S. DOE, Detroit, MI, 2012. https://www.energy.gov/sites/prod/files/2014/03/f8/deer12_maranville.pdf.

[56] E. Wikner, T. Thiringer, Extending Battery Lifetime by Avoiding High SOC, Appl. Sci. . 8 (2018). doi:10.3390/app8101825.

[57] G. Suri, S. Onori, A control-oriented cycle-life model for hybrid electric vehicle lithium-ion batteries, Energy. 96 (2016) 644–653. doi:https://doi.org/10.1016/j.energy.2015.11.075.

[58] G. Suri, S. Onori, A control-oriented cycle-life model for hybrid electric vehicle lithium-

ion batteries, Energy. 96 (2016) 644–653. doi:https://doi.org/10.1016/j.energy.2015.11.075.

[59] U.S. Department of Transportation Federal Highway Administration, 2017 National Household Travel Survey (NHTS), (n.d.). http://nhts.ornl.gov (accessed September 20, 2021).

[60] NOAA, Climate Data Online: Dataset Discovery, Natl. Cent. Environ. Inf. (2023). https://www.ncdc.noaa.gov/cdo-web/datasets (accessed May 4, 2023).

[61] P. Dubey, G. Pulugundla, A.K. Srouji, Direct Comparison of Immersion and Cold-Plate Based Cooling for Automotive Li-Ion Battery Modules, Energies. 14 (2021). doi:10.3390/en14051259.